Journal of Solid State Chemistry 197 (2013) 447–455

Contents lists available at SciVerse ScienceDirect

Journal of Solid State Chemistry

journal homepage: www.elsevier.com/locate/jssc

Crystal structure, morphotropic phase transition and luminescence in the new cyclosilicates $Sr_3R_2(Si_3O_9)_2$, R=Y, Eu–Lu

Alexander P. Tyutyunnik, Ivan I. Leonidov*, Ludmila L. Surat, Ivan F. Berger, Vladimir G. Zubkov

Institute of Solid State Chemistry, UB RAS, 620990 Ekaterinburg, Russian Federation

ARTICLE INFO

Article history:
Received 18 July 2012
Received in revised form
5 September 2012
Accepted 9 September 2012
Available online 16 September 2012

Keywords:
Rietveld refinement
X-ray diffraction
Silicates
Luminescence

ABSTRACT

A new series of promising luminescent materials, cyclosilicates $Sr_3R_2(Si_3O_9)_2$, R=Y, Eu–Lu, has been synthesized via a solid-state reaction. X-ray and neutron powder diffraction studies show that these oxides crystallize in the monoclinic crystal system (S.G. *C2/c*, $Z=4$) and have a morphotropic phase transition between Er and Tm compounds followed by a step-like change of the unit cell constants. Isolated $[Si_3O_9]$ rings located in layers are basic building units and stack with Sr/R layers along the $[1\,0\,\overline{1}]$ direction. The rare earth atoms are distributed among three independent Sr/R sites coordinated by 8, 7 and 6 oxygen atoms, and the Sr-R populations change from mixed to 0.5/0.5 over site (1) and full occupation of sites (2) and (3) by Sr and R, respectively, at the transition. Changes of the conformation and mutual arrangement of $[Si_3O_9]$ rings, as well as exchange of oxygen atoms from the first and the second coordination sphere of two Sr/R sites also feature the phase transition. Luminescence in $Sr_3Y_2(Si_3O_9)_2$:Eu^{3+} under ultraviolet (UV) excitation has been discussed.

1. Introduction

In the past decades, phosphors with ultraviolet (UV) excitation for plasma display panels (PDPs), Hg-free lamps and LCD backlight applications and their fundamental research have received much attention [1–4]. Many reports on compounds in $CaO–Y_2O_3–SiO_2$ system have been published because it is a basic and important system for inorganic luminescent materials with high thermal and chemical stability [5–11]. Crystal structures of quaternary compounds $Ca_3Y_2(SiO_4)_3$ [12,13], $Ca_2Y_2Si_2O_9$ [14], $Ca_2Y_8(SiO_4)_6O_2$ [15,16], $Ca_3Y_6(SiO_4)_6$ [16], $Ca_4Y_6(SiO_4)_6O$ [16] and $Ca_3Y_2(Si_3O_9)_2$ [17,18] comprise either discrete SiO_4 tetrahedra ($Ca_3Y_2(SiO_4)_3$, $Ca_2Y_8(SiO_4)_6O_2$), or Si_2O_7 pyrogroups ($Ca_2Y_2Si_2O_9$), or $[Si_3O_9]$ rings ($Ca_3Y_2(Si_3O_9)_2$) [19]. Luminescence properties of $Ca_3Y_2(SiO_4)_3$, $Ca_2Y_2Si_2O_9$, $Ca_2Y_8(SiO_4)_6O_2$, and $Ca_4Y_6(SiO_4)_6O$ doped with lanthanide ions have been discussed in numerous previous papers [20–35]. The energy transfer $Ce^{3+} \rightarrow Tb^{3+}$ in $Ca_3Y_2(Si_3O_9)_2$:Ce^{3+},Tb^{3+} and room temperature and 10 K luminescence in $Ca_3Y_2(Si_3O_9)_2$:Tb^{3+} under VUV-UV synchrotron radiation excitation have been reported by two research groups [36,37].

Most of quaternary phases in the $R_2O_3–SrO–SiO_2$ system (*R*—rare earth ion) have an apatite-type structure [38–43]. Another crystal structure of the mixed-framework trisilicate $SrY_2Si_3O_{10}$ contains slightly curved Si_3O_{10} and Y_2O_{11} structural units [44]. There are only a few modifications of $Sr_3(Si_3O_9)$ among cyclosilicates in this system with $[Si_3O_9]$ rings located in layers alternating with strontium cations layers [8,45–47] and the high-pressure δ'-phase $Sr_4(Si_4O_{12})$ with tetra-cycles $[Si_4O_{12}]$ [8]. The hexagonal $La_3F_3[Si_3O_9]$, closely related to this system, has ideal tri-cycles [48], $Sr_8(Si_4O_{12})Cl_8$ and $Eu_2Cl_2(SiO_3)$ have tetra-cycles [49,50] and $Na_2Sr(Si_2O_6)$ has hexa-cycles [51] in the crystal structure. $Ca_3Y_2(Si_3O_9)_2$ derived from a wadeite α-$CaSiO_3$ (pseudowollastonite, a high-temperature polymorph of $CaSiO_3$ [52]) has been studied in detail by Yamane et al. [17] and its structure has been compared with structures of closely related silicates. This compound crystallizes in the space group *C2/c* ($Z=4$). Ca and Y atoms are in eight-, seven- and sixfold coordination sites between the layers of $[Si_3O_9]$ rings. The average Si–Si distances 3.035 Å were reported to be consistent with the non-bonding distance $2R=3.06$ Å for regular SiO_4 tetrahedra [53], which O'Keeffe and Hyde used to explain the rarity of ternary SiO_4 rings, i.e. $[Si_3O_9]$, in silicate structures and the anomalously long strained Si–O bonds observed in the 3-rings. In this paper, we report crystal structure, morphotropic phase transition (MPT [54]) in the new group of cyclosilicates $Sr_3R_2(Si_3O_9)_2$, R=Y, Eu–Lu, and visible luminescence in $Sr_3Y_2(Si_3O_9)_2$:Eu^{3+} under UV excitation.

2. Materials and methods

A series of silicates $Sr_3R_2(Si_3O_9)_2$, R=Y, Eu, Gd, Tb, Dy, Ho, Er, Tm, Yb, Lu, was prepared via a solid-state reaction route at ambient pressure from stoichiometric mixtures of $SrCO_3$ (99.95%), R_2O_3 (99.98%) and amorphous SiO_2 (99.995%). The samples were pressed into pellets, placed in alumina boats and annealed at $T=950$ °C for 1–2 h, for $SrCO_3$ decarbonization to SrO,

* Corresponding author.
E-mail address: ivanleonidov@ihim.uran.ru (I.I. Leonidov).

0022-4596/$ - see front matter © 2012 Elsevier Inc. All rights reserved.
http://dx.doi.org/10.1016/j.jssc.2012.09.009

and then at $T=1300\,^{\circ}C$ for 150–200 h in air with intermediate regrinding in an agate mortar, and cooled down with the furnace. Terbium silicate was synthesized in the neutral atmosphere (Ar). The homogeneous solid solution $Sr_3Y_{2-x}Eu_x(Si_3O_9)_2$, $x=0.25$–2, was prepared from stoichiometric mixtures of $Sr_3Y_2(Si_3O_9)_2$ and $Sr_3Eu_2(Si_3O_9)_2$ samples by the same thermal processing.

The single-phase character of the final products was checked by X-ray powder diffraction. All X-ray powder diffraction (XRD) patterns were collected on a STADI-P automated diffractometer (STOE) equipped with a linear mini-PSD detector using Cu Kα_1 radiation in the 2θ range from 5° to 120° with a step of 0.02°. Polycrystalline silicon ($a=5.43075(5)$ Å) was used as an external standard. Possible impurity phases were checked by comparing their XRD patterns with those in the PDF2 database (Powder diffraction file, ICDD, release 2009). Since scattering powers of Sr and Y in XRD experiments are very close, the neutron diffraction measurements of $Sr_3Y_2(Si_3O_9)_2$ have been carried out at room temperature on a D7A setup of the IVV 2M reactor (Zarechny, Russia) in the 2θ range from 10° to 125° with a 0.05° step and neutron wavelength $\lambda=1.5275$ Å. The crystal structure refinement of $Sr_3R_2(Si_3O_9)_2$, R=Y, Eu–Lu, was carried out with the GSAS program suite using XRD data; in case of $Sr_3Y_2(Si_3O_9)_2$ both X-ray and neutron diffraction data were used simultaneously [55]. The peak profiles were fitted with a pseudo-Voigt function, $I(2\theta)=x{*}L(2\theta)+(1-x){*}G(2\theta)$ (where L and G are the Lorentzian and Gaussian part, respectively). The angular dependence of the peak width was described by the relation $(FWHM)^2=Utg^2\theta+Vtg\theta+W$, where $FWHM$ is the full line width at half maximum. The background level was described by a combination of 36-order Chebyshev polynomials. The absorption correction function for a flat plate sample in transmission geometry was applied [55].

The room temperature photoluminescence (PL) and photoluminescence excitation (PLE) spectra were recorded on a Varian Cary Eclipse fluorescence spectrophotometer coupled to a personal computer with Varian software and supplied with a 75 kW Xenon lamp as excitation source (pulse length $\tau=2$ µs, pulse frequency $\nu=80$ Hz, wavelength resolution 0.5 nm; PMT Hamamatsu R928).

3. Results and discussion

3.1. Structural analysis

The XRD patterns of $Sr_3R_2(Si_3O_9)_2$, R=Y, Eu–Lu, can be indexed with monoclinic unit cells $C2/c$ (S.G. No. 15, $Z=4$), with the constants following the linear dependence upon the crystal radius [56] of rare earth ions until MPT between Er and Tm compounds accompanied by a step-like decrease in a, c and V and an increase in b and β (Table 1, Fig. 2). Since the nominal composition of the synthesized $Sr_3R_2(Si_3O_9)_2$ compounds corresponds to the formula of $Ca_3Y_2(Si_3O_9)_2$, the latter was used as a starting model for the crystal structure refinement [17]. Structural data, atomic coordinates and isotropic thermal parameters are listed in Tables 1 and 2. All data for $Sr_3Y_2(Si_3O_9)_2$ are placed among those for rare earth silicates according to crystal radius. The mass fractions of impurity phases used in the full-profile fitting are shown as m. % (Table 1). The fractions of strontium in the Sr(2)/R(2) sites for Tm, Yb and Lu were found to exceed 1.0 less than in three standard deviations and were fixed to 1.0, the fractions in the Sr(1)/R(1) and Sr(3)/R(3) sites were constrained to keep the overall composition $Sr_3R_2(Si_3O_9)_2$. Fig. 1(a, b) displays experimental, calculated and difference XRD patterns for the Er and Tm samples, respectively. The selected interatomic distances, bond angles and the specific distances in $Sr_3R_2(Si_3O_9)_2$, R=Y, Eu–Lu, are listed in Tables 3 and 4. The difference in neutron cross-section for Sr and Y, 0.702 and 0.775,

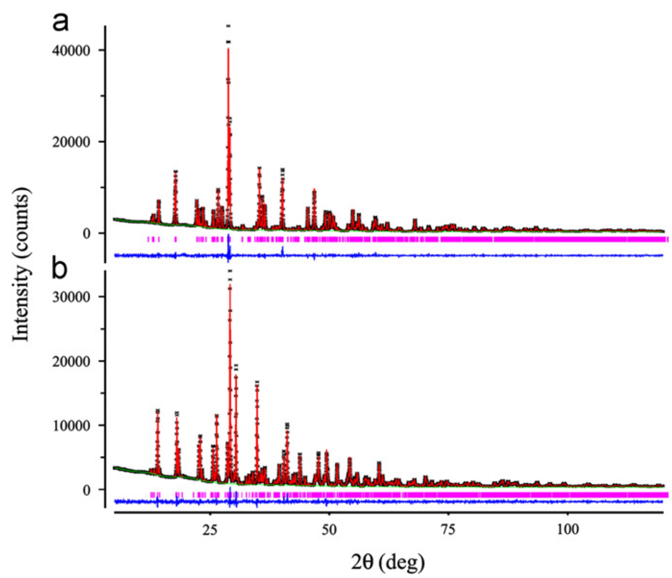

Fig. 1. Observed (crosses), calculated (solid line) and difference (bottom) XRD patterns for $Sr_3Er_2(Si_3O_9)_2$ (a) and $Sr_3Tm_2(Si_3O_9)_2$ (b).

Table 1
Structural data for $Sr_3R_2(Si_3O_9)_2$, R=Y, Eu–Lu.

Parameter	Eu	Gd	Tb	Dy	Y	Ho	Er	Tm	Yb	Lu
Crystal system	Monoclinic									
Space group	$C2/c$ (No. 15)									
Cell constants										
a, Å	13.6036(9)	13.5863(9)	13.5492(9)	13.5396(9)	13.5220(9)	13.5206(9)	13.5027(9)	13.3937(9)	13.3924(9)	13.3777(9)
b, Å	8.0219(7)	8.0130(7)	8.0005(7)	7.9894(7)	7.9750(7)	7.9798(7)	7.9741(7)	8.2608(7)	8.2542(7)	8.2518(7)
c, Å	14.9987(9)	14.9630(9)	14.8909(9)	14.8601(9)	14.8353(9)	14.8240(9)	14.7791(9)	13.7065(9)	13.6825(9)	13.6627(9)
β, deg	89.526(6)	89.698(6)	89.837(6)	90.004(6)	90.157(6)	90.161(6)	90.297(6)	93.328(6)	93.394(6)	93.477(6)
V, Å^3	1636.7	1629.0	1614.2	1607.5	1599.8	1599.4	1591.3	1514.0	1509.9	1505.4
Z	4	4	4	4	4	4	4	4	4	4
D_{calcd}, g·cm^{-3}	4.151	4.214	4.260	4.311	3.722	4.356	4.401	4.637	4.687	4.717
m.% $SrSiO_3$	0.0	1.0	0.0	0.5	0.0	0.0	0.8	0.0	0.0	0.0
m.% $Sr_2R_8O_2(SiO_4)_6$	2.9	1.1	1.5	0.0	0.0	0.8	0.5	0.0	0.0	0.0
R_{wp}	1.55	1.32	2.12	1.97	3.92	4.43	5.06	4.83	4.59	4.71
R_p	1.18	0.99	1.62	1.49	3.34	3.37	3.89	3.60	3.35	3.53
$R(F^2)$ (%)	3.85	3.74	4.95	3.67	3.29	3.15	2.78	2.71	2.48	2.43
χ^2	1.672	2.026	1.911	1.810	3.775	2.776	3.323	3.195	5.378	3.125

Note: For neutron data of $Sr_3Y_2(Si_3O_9)_2$: $R_{wp}=2.21\%$, $R_p=1.75\%$, $R(F^2)=4.44\%$.